Quantum Mechanical Studies of the Photodissociation of Carbonylheme Complexes

Ahmad Waleh* and Gilda H. Loew*

Contribution from the Molecular Theory Laboratory, The Rockefeller University, 701 Welch Road, Palo Alto, California 94304. *Received July 27, 1981*

Abstract: In order to identify the photoactive excited states involved in the photodissociation of carbon monoxyhemoproteins, the excited-state energies of carbonylheme complexes as a function of iron–ligand distance were calculated by using an INDO–SCF–CI method. Complexes with both bent and linear CO geometries, corresponding to hemoproteins and model compounds, respectively, were investigated. For both types of complexes, only excited states involving $d\pi \rightarrow d_{z^2}^*$ and $d_{x^2-y^2} \rightarrow d_{z^2}^*$ transitions showed a significant decrease in energy with increasing iron–ligand distance, making them the definitive candidates for the photoactive states. Of the two, the $d\pi \rightarrow d_{z^2}^*$ states with significant oscillator strength and more bond weakening characteristics appear to be the main photodissociating state. The previously suggested possibility that states resulting from $\pi \rightarrow \pi^*$ transitions are directly photodissociating is ruled out. Our results also show that triplet partners of the $d\pi \rightarrow d_{z^2}^*$ states need not be involved in the initiation of dissociation. Bending of the CO bond from the axis normal to the heme plane, corresponding to a possible intact protein geometry, significantly lowers the energies of the excited states corresponding to the $d\pi \rightarrow d_{z^2}^*$ and $d_{x^2-y^2} \rightarrow d_{z^2}^*$ transitions. The calculated energies of the singlet $d\pi \rightarrow d_{z^2}^*$ transitions in the bent carbonylheme complex are 15 700 and 18 500 cm^{-1}, in excellent agreement with circular dichroism spectra, and form the basis of a proposed mechanism of photodissociation which is consistent with the observed high and wavelength-independent quantum yield of CO photodissociation of hemoproteins. The implication of the results for model compounds, with presumed linear CO geometry, is also discussed.

Photodissociation of ferrous liganded complexes of hemoproteins has been the subject of active interest over the last 20 years and particularly in recent years due to advances made in pulse laser technology. Even though the photolability of CO in MbCO [Abbreviations: MbCO, carbon monoxymyoglobin; HbCO, carbon monoxyhemoglobin; Hb, deoxyhemoglobin.] was observed by Haldane and Lorrain Smith[1] as early as 1896, it was not until nearly 60 years later that additional photolabile ligands, specifically CN^-, O_2, and NO, were identified.[2,3] The renewed interest in photodissociation stems from the fact that it has become increasingly clear that the understanding of the metal–ligand bond breaking process, which is possibly the first and rate-limiting step in the ligand dissociation, is essential to gaining insight into the other primary molecular events, such as electronic or tertiary structural changes which precede, and eventually lead to, the quaternary conformational changes in hemoglobin that trigger cooperativity.

One of the central problems of photodissociation is the identification of the photoactive state(s) which mechanistically participate in the ligand dissociation. An enigmatic feature of photodissociation in hemoproteins is the variation in quantum yield for different ligands[3-6] ranging from the highly photosensitive MbCO[5,7-10] with quantum yield, ϕ_{CO}, near unity to minimally sensitive O_2 and NO derivatives of hemoglobin with ϕ_{O_2} and ϕ_{NO} of 0.03 and 0.003, respectively.[3,5] Moreover, the quantum yield of photodissociation is shown to depend on the nature of the protein[4,7,9,10] as well as on such factors as ionic strength,[9] protein concentration,[9] and temperature.[5] Another feature of interest is the observation of the wavelength independence of quantum yield in MbCO over the range 280–570 nm[8] and probably as far into the red as 620 nm.[6] Photodissociation also occurs in liganded model heme complexes.[6,7,11,12]

With the development of pulsed lasers, attention has been progressively more focused on the molecular events in the time range of microseconds to picoseconds after photodissociation. In this regard, time-resolved absorption,[13-26] CARS,[27] and resonance Raman[28-33] spectroscopy of the photolyzed oxy- and carbon

(1) J. S. Haldane and J. Lorrain Smith, *J. Physiol.*, **20**, 497 (1896).
(2) D. Keilin and E. F. Hartree, *Biochem. J.*, **61**, 153 (1955).
(3) Q. H. Gibson and S. Ainsworth, *Nature (London)*, **180**, 1416 (1957).
(4) M. Brunori, G. M. Giacometti, E. Antonini, and J. Wyman, *Proc. Natl. Acad. Sci. U.S.A.*, **70**, 3141 (1973).
(5) W. A. Saffran and Q. H. Gibson, *J. Biol. Chem.*, **252**, 7955 (1977).
(6) B. M. Hoffman and Q. H. Gibson, *Proc. Natl. Acad. Sci. U.S.A.*, **75**, 21 (1978).
(7) T. Bücher and E. Negelein, *Biochem. Z.*, **311**, 163 (1941).
(8) T. Bücher and J. Kaspers, *Biochim. Biophys. Acta*, **1**, 21 (1947).
(9) R. W. Noble, M. Brunori, J. Wyman, and E. Antonini, *Biochemistry*, **6**, 1216 (1967).
(10) C. Bonaventura, J. Bonaventura, E. Antonini, M. Brunori, and J. Wyman, *Biochemistry*, **12**, 3424 (1973).
(11) M. H. Smith, *Biochem. J.*, **73**, 90 (1959).
(12) C. K. Chang and T. G. Traylor, *Proc. Natl. Acad. Sci. U.S.A.*, **72**, 1166 (1975).
(13) R. H. Austin, K. W. Beeson, L. Eisenstein, H. Frauenfelder, and I. C. Gunsalus, *Biochemistry*, **14**, 5355 (1975).
(14) N. Alberding, R. H. Austin, S. S. Chan, L. Eisenstein, H. Frauenfelder, I. C. Gunsalus, and T. M. Nordlund, *J. Chem. Phys.*, **65**, 4701 (1976).
(15) N. Alberding, S. S. Chan, L. Eisenstein, H. Frauenfelder, D. Good, I. C. Gunsalus, T. M. Nordlund, M. F. Perutz, A. H. Reynolds, and L. B. Sorensen, *Biochemistry*, **17**, 43 (1978).
(16) D. Beece, L. Eisenstein, H. Frauenfelder, D. Good, M.c. Marden, L. Reinisch, A. H. Reynolds, L. B. Sorensen, and K. T. Yue, *Biochemistry*, **18**, 3421 (1979).
(17) C. A. Sawicki and Q. H. Gibson, *J. Biol. Chem.*, **251**, 1533 (1976).
(18) B. Alpert, S. El Mohsni, L. Lindqvist, and F. Tfibel, *Chem. Phys. Lett.*, **64**, 11 (1979).
(19) C. V. Shank, E. P. Ippen, and R. Bersohn, *Science (Washington, D.C.)*, **193**, 50 (1976).
(20) L. J. Noe, W. G. Eisert, and P. M. Rentzepis, *Proc. Natl. Acad. Sci. U.S.A.*, **75**, 573 (1978).
(21) W. G. Eisert, E. O. Degenkolb, L. J. Noe, and P. M. Rentzepis, *Biophys. J.*, **25**, 455 (1979).
(22) A. H. Reynolds, S. D. Rand, and P. M. Rentzepis, *Proc. Natl. Acad. Sci. U.S.A.*, **78**, 2292 (1981).
(23) D. A. Duddell, R. J. Morris, and J. T. Richards, *Biochim. Biophys. Acta*, **621**, 1 (1980).
(24) D. A. Duddell, R. J. Morris, N. J. Muttucumaru, and J. T. Richards, *Photochem. Photobiol.*, **31**, 479 (1980).
(25) B. I. Greene, R. M. Hochstrasser, R. B. Weisman, and W. A. Eaton, *Proc. Natl. Acad. Sci. U.S.A.*, **75**, 5255 (1978).
(26) D. A. Chernoff, R. M. Hochstrasser, and A. W. Steele, *Proc. Natl. Acad. Sci. U.S.A.*, **77**, 5606 (1980).
(27) R. F. Dallinger, J. R. Nestor, and T. G. Spiro, *J. Am. Chem. Soc.*, **100**, 6251 (1978).
(28) K. B. Lyons, J. M. Friedman, and P. A. Fleury, *Nature (London)*, **275**, 565 (1978).
(29) J. M. Friedman and K. B. Lyons, *Nature (London)*, **284**, 570 (1980).
(30) J. Terner, T. G. Spiro, M. Nagumo, M. F. Nicol, and M. A. El-Sayed, *J. Am. Chem. Soc.*, **102**, 3238 (1980).
(31) J. Terner, J. D. Stong, T. G. Spiro, M. Nagumo, M. Nicol, and M. A. El-Sayed, *Proc. Natl. Acad. Sci. U.S.A.*, **78**, 1313 (1981).
(32) M. Coppey, H. Tourbez, P. Valat, and B. Alpert, *Nature (London)*, **284**, 568 (1980).

0002-7863/82/1504-2346$01.25/0

monoxyhemoproteins have been utilized to study the dynamics of the ligand dissociation and its subsequent recombination. These experiments have yielded valuable information about the nature and characteristics of the transient and/or intermediate species of photodissociation leading to the formation of stable deoxy species. However, in spite of the picosecond probing of the photodissociation site, the exact nature of the photoactive excited state(s) leading to ligand dissociation is far from being resolved.

A number of mechanisms have been proposed to explain photodissociation in hemoproteins.[6,19-22,25,26,30,31,34] However, none has led to unequivocal identification of photoactive excited state(s) that mechanistically explains the ready photolability of both CO and O_2 together with the contrasting difference in their quantum yield of photodissociation.

The iterative extended Hückel theory (IEHT) of Zerner et al.[34] has been used to interpret the experimental results in terms of populating the excited states corresponding to $\pi \rightarrow \pi^*$ transitions (Q band) of the porphyrin followed by a radiationless decay into a $d\pi \rightarrow d_{z^2}{}^*$ state or its triplet partner.[19-21,30] The latter transition has been suggested as a likely photoactive excited state because of its presumed bond weakening ability,[34] and the $\pi \rightarrow \pi^*$ transition is invoked to explain the high quantum yield of CO as well as its wavelength independence in the excitation range of 280–620 nm.[6,8] The underlying assumption in these arguments is that, at least, the triplet $d\pi \rightarrow d_{z^2}{}^*$ transition lies below the Q band. Alternatively, it has been proposed[6] that photodissociation might occur directly from the lowest singlet $\pi \rightarrow \pi^*$ (Q) or from its triplet partner after intersystem crossing. The previous theoretical studies of oxy- and carbonylheme complexes using extended Hückel,[35-37] ab initio,[38-41] and PPP[42,43] methods have not addressed the problem of photodissociation directly and thus have not been able to distinguish definitively among the various suggested mechanisms.

We have recently reported the calculated optical spectra of oxy- and carbonylheme complexes.[44-46] As a logical extension of this work, we have begun theoretical studies designed to definitively establish the identification of their photoactive excited states. The main criterion we use to identify such states is that they have decreasing energy as a function of increasing iron–ligand distance with no barrier to dissociation. In the work presented here, we report a detailed determination of the energy profile of the excited states of carbonylheme complexes as a function of iron–ligand distance with no change in spin or conformation. The studies were made for complexes with linear and bent CO geometries representing model compounds and protein complexes, respectively. Complimentary studies for an oxyheme complex are presented in the following companion paper.[47]

Table I. Ground-State Orbital Description of Linear Carbonylheme Complex at Iron-Carbon Distances of 1.77 and 2.37 Å[a]

orbital no.	Fe–C = 1.77 Å	Fe–C = 2.37 Å
92	(90% Imidσ, 3% d_{z^2})*	(56% d_{xy}, 41% Porphσ)*
91	100% a_{1u}*	(93% Imidσ, 1% d_{z^2})*
90	(59% d_{xy}, 37% Porphσ)*	100% a_{1u}*
89	(93% e_g, 3% COπ, 2% d_{z^2})*	99% e_g*
88	(88% e_g, 5% d_{z^2}, 3% COπ)*	99% e_g*
87	(43% d_{z^2}, 21% Imidσ, 14% Porphσ, 12% Porphπ, 7% COσ)*	(63% d_{z^2}, 14% Imidσ, 6% Porphσ, 6% COσ)*
86	(65% COπ, 21% Imidπ, 7% dπ)*	99% b_{1u}*
85	(55% COπ, 37% b_{1u}, 5% dπ)*	99% Imidπ*
84	(65% b_{1u}, 30% COπ, 3% dπ)*	(89% Imidπ, 10% COπ, 1% dπ)*
83	(79% Imidπ, 18% COπ, 1% dπ)*	100% b_{2u}*
82	100% b_{2u}*	(98% COπ, 1% dπ)*
81	(99% Imidπ, 1% COπ)*	(88% COπ, 11% Imidπ)*
80	(98% e_g, 2% dπ)*	(98% e_g, 1% dπ)*
79	(98% e_g, 2% dπ)*	(99% e_g, 1% dπ)*
78	100% a_{1u}	100% a_{1u}
77	97% a_{2u}	98% a_{2u}
76	62% dπ, 31% e_g, 4% COπ	71% dπ, 26% e_g
75	62% dπ, 33% e_g, 4% COπ	70% dπ, 27% e_g
74	96% $d_{x^2-y^2}$	96% $d_{x^2-y^2}$
73	70% Imidπ, 30% b_{1u}	75% Imidπ, 25% b_{1u}
72	93% a_{2u}, 3% COπ	88% b_{1u}, 11% Imidπ
71	78% b_{1u}, 22% Imidπ	92% a_{2u}, 6% Imidπ
70	98% e_g	93% e_g, 3% dπ
69	99% e_g	100% e_g
68	63% e_g, 17% dπ, 15% Imidπ, 4% COπ	71% e_g, 14% dπ, 13% Imidπ
67	70% e_g, 23% dπ, 6% dπ	74% e_g, 24% dπ, 1% COπ

[a] Only the orbitals involved in the electronic transitions of below about 30 000 cm^{-1} are shown. Except for iron d and COπ orbitals, all contributions below 5% are neglected. All symmetry designations refer to prophyrin π orbitals in D_{4h} symmetry.

Method

The calculations were carried out by using an INDO (intermediate neglect of differential overlap) program[48-51] which allows for the treatment of transition-metal complexes and the inclusion of extensive configuration interactions. The details of the program are described elsewhere.[44,45,52]

The geometry of the model carbonylheme complexes used in this study is the same as those used in the calculation of the carbonylheme spectra[45] except for variations in the Fe–CO distance along the axis perpendicular to the plane of the porphyrin. In the coordinate system chosen, the pyrole nitrogen atoms bisect the *xy* axes, and therefore, the d_{xy} orbital becomes the "e_g" partner of d_{z^2}. Two sets of calculations were carried out, one for linear and one for bent Fe–C–O geometries, corresponding to the expected geometries of model carbonylheme compounds[53,54] and carbon monoxyhemoproteins,[55-60] respectively. In each set, the

(33) W. H. Woodruff and S. Farquharson, *Science (Washington, D.C.)*, **201**, 831 (1978).
(34) M. Zerner, M. Gouterman, and H. Kobayashi, *Theor. Chim. Acta*, **6**, 363 (1966).
(35) R. F. Kirchner and G. H. Loew, *J. Am. Chem. Soc.*, **99**, 4649 (1977).
(36) G. H. Loew and R. F. Kirchner, *Int. J. Quantum Chem., Quantum. Biol. Symp.*, **5**, 403 (1978).
(37) W. A. Eaton, L. K. Hanson, P. J. Stephens, J. C. Sutherland, and J. B. R. Dunn, *J. Am. Chem. Soc.*, **100**, 4991 (1978).
(38) A. Dedieu, M. M. Rohmer, M. Bernard, and A. Veillard, *J. Am. Chem. Soc.*, **98**, 3717 (1976).
(39) A. Dedieu, M. M. Rohmer, H. Veillard, and A. Veillard, *Bull. Soc. Chim. Belg.*, **85**, 953 (1976).
(40) A. Dedieu, M. M. Rohmer, and A. Veillard in "Metal-Ligand Interactions in Organic Chemistry and Biochemistry", Part 2, B. Pullman and N. Goldblum, Eds., D. Reidel, Dordrecht, Holland, 1977, p 101.
(41) A. Dedieu, M. M. Rohmer, H. Veillard, and A. Veillard, *Nouv. J. Chim.*, **3**, 653 (1979).
(42) B. H. Huynh, D. A. Case, and M. Karplus, *J. Am. Chem. Soc.*, **99**, 6103 (1977).
(43) D. A. Case, B. H. Huynh, and M. Karplus, *J. Am. Chem. Soc.*, **101**, 4433 (1979).
(44) G. H. Loew, Z. S. Herman, and M. C. Zerner, *Int. J. Quantum Chem.*, **18**, 481 (1980).
(45) Z. S. Herman, G. H. Loew, and M. M. Rohmer, *Int. J. Quantum Chem., Quantum Biol. Symp.*, **7**, 137 (1980).
(46) G. H. Loew and M. M. Rohmer, *J. Am. Chem. Soc.*, **102**, 3655 (1980).
(47) A. Waleh and G. H. Loew, *J. Am. Chem. Soc.*, following paper in this issue.
(48) J. Ridley and M. Zerner, *Theor. Chim. acta*, **32**, 111 (1973).
(49) J. E. Ridley and M. C. Zerner, *Theor. Chim. Acta*, **42**, 223 (1976).
(50) A. D. Bacon, Ph.D. dissertation, Department of Chemistry, University of Guelph, Canada, 1976.
(51) A. D. Bacon and M. C. Zerner, *Theor. Chim. Acta*, **53**, 21 (1979).
(52) M. C. Zerner, G. H. Loew, R. F. Kirchner, and U. T. Mueller-Westerhoff, *J. Am. Chem. Soc.*, **102**, 589 (1980).
(53) J. L. Hoard, "Stereochemistry of Porphyrins and Metalloporphyrins" in "Porphyrins and Metalloporphyrins", K. M. Smith, Ed., Elsevier, Amsterdam, 1975, pp 351–371.
(54) S. M. Peng and J. A. Ibers, *J. Am. Chem. Soc.*, **98**, 8032 (1976).
(55) R. Huber, O. Epp, and H. Formanek, *J. Mol. Biol.*, **52**, 349 (1970).
(56) J. C. Norvell, A. C. Nunes, and B. P. Schoenborn, *Science (Washington, D.C.)*, **190**, 568 (1975).
(57) E. A. Padlan and W. E. Love, *J. Biol. Chem.*, **249**, 4067 (1975).
(58) E. J. Heidner, R. C. Ladner, and M. F. Perutz, *J. Mol. Biol.*, **104**, 707 (1976).

Table II. Calculated Excited States of Linear Carbonylheme Complex below 30 000 cm^{-1} as a Function of Iron-Carbon Distance

Fe-C = 1.77 Å		Fe-C = 2.17 Å		Fe-C = 2.37 Å	
frequency,[a] cm^{-1}	major components	frequency, cm^{-1}	major components	frequency, cm^{-1}	major components
				14 771	$(d\pi,\pi) \rightarrow d_{z^2}^*; d_{xy}^*$ (94%; 4%)
				15 017	$(d\pi,\pi) \rightarrow d_{z^2}^*; d_{xy}^*$ (91%; 4%)
16 915 (0.035; xy)	$a_{1u}; a_{2u} \rightarrow e_g^*$ (56%, 41%)	17 094	$a_{1u}; a_{2u} \rightarrow e_g^*$ (58%; 39%)	17 163	$a_{1u}; a_{2u} \rightarrow e_g^*$ (59%; 38%)
16 967 (0.032; xy)	$a_{1u}; a_{2u} \rightarrow e_g^*$ (56%; 41%)	17 147	$a_{1u}; a_{2u} \rightarrow e_g^*$ (58%; 39%)	17 217	$a_{1u}; a_{2u} \rightarrow e_g^*$ (58%; 39%)
		17 601	$(d\pi,\pi) \rightarrow d_{z^2}^*; d_{xy}^*$ (92%; 7%)		
		17 808	$(d\pi,\pi) \rightarrow d_{z^2}^*; d_{xy}^*$ (90%; 7%)		
				20 094	$d_{x^2-y^2} \rightarrow d_{z^2}^*$ (78%); $(d\pi,\pi) \rightarrow e_g^*$ (19%)
21 944	$(d\pi,\pi) \rightarrow e_g^*$ (57%); $d_{x^2-y^2} \rightarrow d_{xy}^*$ (41%)	21 275	$(d\pi,\pi) \rightarrow e_g^*$ (90%)	21 374	$(d\pi,\pi) \rightarrow e_g^*$ (95%)
22 781	$d_{x^2-y^2} \rightarrow d_{xy}^*$ (55%); $(d\pi,\pi) \rightarrow e_g^*$ (45%)	21 486	$(d\pi,\pi) \rightarrow e_g^*$ (77%); $d_{x^2-y^2} \rightarrow d_{z^2}^*$ (18%)	22 062	$(d\pi,\pi) \rightarrow e_g^*$ (94%)
22 877	$(d\pi,\pi) \rightarrow e_g^*$ (93%)	22 036	$(d\pi,\pi) \rightarrow e_g^*$ (95%)	22 509	$(d\pi,\pi) \rightarrow e_g^*$ (79%); $d_{x^2-y^2} \rightarrow d_{z^2}^*$ (19%)
23 081	$(d\pi,\pi) \rightarrow e_g^*$ (92%)	23 341	$d_{x^2-y^2} \rightarrow d_{xy}^*; d_{z^2}^*$ (85%; 8%); $(d\pi,\pi) \rightarrow e_g^*$ (7%)	23 727	$d_{x^2-y^2} \rightarrow d_{xy}^*$ (97%)
		23 982	$d_{x^2-y^2} \rightarrow d_{z^2}^*; d_{xy}^*$ (66%; 11%); $(d\pi,\pi) \rightarrow e_g^*$ (19%)		
25 089 (0.005; xy)	$(d\pi,\pi) \rightarrow d_{z^2}^*; d_{xy}^*$ (53%; 37%); $d_{x^2-y^2} \rightarrow e_g^*$ (5%)				
25 189 (0.006; xy)	$(d\pi,\pi) \rightarrow d_{z^2}^*; d_{xy}^*$ (52%; 37%); $d_{x^2-y^2} \rightarrow e_g^*$ (7%)				
26 749 (0.002; xy)	$d_{x^2-y^2} \rightarrow e_g^*$ (83%); $(d\pi,\pi) \rightarrow d_{z^2}^*$ (11%)	24 414	$d_{x^2-y^2} \rightarrow e_g^*$ (95%)	24 046	$d_{x^2-y^2} \rightarrow e_g^*$ (97%)
26 847 (0.002; xy)	$d_{x^2-y^2} \rightarrow e_g^*$ (85%); $(d\pi,\pi) \rightarrow d_{z^2}^*$ (9%)	24 531	$d_{x^2-y^2} \rightarrow e_g^*$ (95%)	24 154	$d_{x^2-y^2} \rightarrow e_g^*$ (97%)
27 504 (0.005; z)	$(d\pi,\pi) \rightarrow e_g^*$ (95%)	26 560	$(d\pi,\pi) \rightarrow e_g^*$ (91%)	26 560	$(d\pi,\pi) \rightarrow e_g^*$ (92%)
28 933 (1.958; y)	$a_{1u}; a_{2u} \rightarrow e_g^*$ (38%; 54%)	29 244	$a_{1u}; a_{2u} \rightarrow e_g^*$ (33%; 51%); $(d\pi,\pi) \rightarrow d_{xy}^*$ (5%)	29 465	$a_{1u}; a_{2u} \rightarrow e_g^*$ (31%; 45%)
29 095 (2.054; x)	$a_{1u}; a_{2u} \rightarrow e_g^*$ (37%; 54%)	29 398	$a_{1u}; a_{2u} \rightarrow e_g^*$ (30%; 45%); $(d\pi,\pi) \rightarrow d_{xy}^*$ (12%)	29 623	$a_{1u}; a_{2u} \rightarrow e_g^*$ (28%; 48%); $(d\pi,\pi) \rightarrow d_{xy}^*$ (9%)
30 575 (0.006; xy)	$(d\pi,\pi) \rightarrow d_{xy}^*; d_{z^2}^*$ (60%; 30%); $d_{x^2-y^2} \rightarrow e_g^*$ (6%)	29 663	$(d\pi,\pi) \rightarrow d_{xy}^*$ (71%); $a_{1u}; a_{2u} \rightarrow e_g^*$ (5%; 8%)	29 846	$(d\pi,\pi) \rightarrow d_{xy}^*$ (75%); $a_{1u} \rightarrow CO\pi^*$ (13%)
30 765	$d_{x^2-y^2} \rightarrow d_{z^2}^*$ (85%)				
30 868 (0.002; xy)	$(d\pi,\pi) \rightarrow d_{xy}^*; d_{z^2}^*$ (59%; 31%); $d_{x^2-y^2} \rightarrow e_g^*$ (6%)	29 858	$(d\pi,\pi) \rightarrow d_{xy}^*; d_{z^2}^*$ (83%; 6%)	30 027	$(d\pi,\pi) \rightarrow d_{xy}^*$ (75%); $a_{1u} \rightarrow CO\pi^*$ (16%)

[a] Nonzero oscillator strengths and polarizations are given in parentheses.

ground- and excited-state electron distributions and energies were calculated at four different iron–carbon distances corresponding to the displacement of CO in 0.2-Å steps from an initial Fe–C bonding distance of 1.77–2.37 Å. Similar calculations were also performed with iron out of the porphyrin plane by 0.24 Å while keeping the iron–imidazole distance constant.

SCF–MO–LCAO level calculations were performed on each of the geometries described above by using an INDO/1 approximation with the two-center repulsion integrals evaluated using an empirical Weiss–Mataga–Nishimoto formula.[61,62] Excited-state energies were calculated by performing single excitation configuration interaction (CI) computations on the SCF level eigenvectors. A total of 206 such configurations were used, in each case, corresponding to excitations from 14 highest occupied orbitals into 14 lowest virtual orbitals and a small set of 10 configurations involving a few remaining low-lying orbitals with minor iron d characters.

Results

Table I shows the calculated ground-state molecular orbital descriptions of linear carbonylheme complex at iron–carbon distance of 1.77 Å (bonding) and also at 2.37 Å for comparison. The main effect of lengthening the Fe–CO distance is an increase in the d_{z^2} contribution to the antibonding virtual orbital 87, making it a more localized d_{z^2} orbital. There is also a parallel decrease of COπ character in both bonding (67, 68, 75, and 76) and antibonding (83–89) orbitals. Table II displays the major details of the calculated excited states of linear carbonylheme complex below about 31 000 cm^{-1} at iron–carbon distances of 1.77, 2.17, and 2.37 Å. The calculated results at 1.97 Å smoothly fall between those at 1.77 and 2.17 Å and are omitted from Table II. A simplified scaled diagramatic representation of the excited-state energies at all four iron–carbon distances is also shown in Figure 1 where only the states which show large variations in energy are identified. The most striking feature of these results is the lowering of the energies of the states corresponding to the $d\pi \rightarrow d_{z^2}^*$ transitions from 25 000 and 31 000 cm^{-1} at Fe–C distance of 1.77 Å to about 21 000 cm^{-1} at 1.97 Å and to below 15 000 cm^{-1} at 2.37 Å. In contrast, the states corresponding to the $\pi \rightarrow \pi^*$ transitions of the Q and Soret bands do not display any dissociative character and, indeed, show a slight increase in energy with the increasing iron–carbon distance. The only other state displaying a significant dissociative profile is the one corresponding to the $d_{x^2-y^2} \rightarrow d_{z^2}^*$ which is lowered from about 31 000 to about 20 000 cm^{-1} over the full range of CO displacement studied. No other excited state displays a lowering of more than 3000 cm^{-1}.

Similar calculations were also carried out with iron out of the porphyrin plane toward the imidazole ligand by 0.24 Å, in a $S = 0$ state, at three iron–carbon distances (1.77, 2.01, and 2.37 Å). The resulting excited-state energy profiles were qualitatively similar to those shown in Table II and Figure 1. However, the

(59) P. W. Tucker, S. E. V. Phillips, M. F. Perutz, R. A. Houtchens, and W. S. Caughey, *Proc. Natl. Acad. Sci. U.S.A.*, **75**, 1076 (1978).
(60) J. M. Baldwin, *J. Mol. Biol.*, **136**, 103 (1980).
(61) K. Weiss, unpublished.
(62) N. Mataga and K. Nishimoto, *Z. Phys. Chem. (Wiesbaden)*, **13**, 140 (1957).

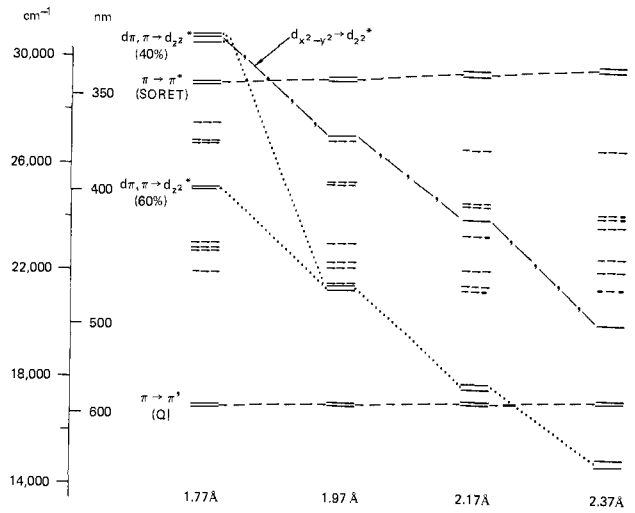

Figure 1. Simplified scaled diagramatic representation of the excited-state energies of the linear carbonylheme complex at iron–carbon distances of 1.77, 1,97, 2.17, and 2.37 Å showing correlation between similar photodissociating states. The $\pi \rightarrow \pi^*$ transitions of the Soret and Q bands are also identified.

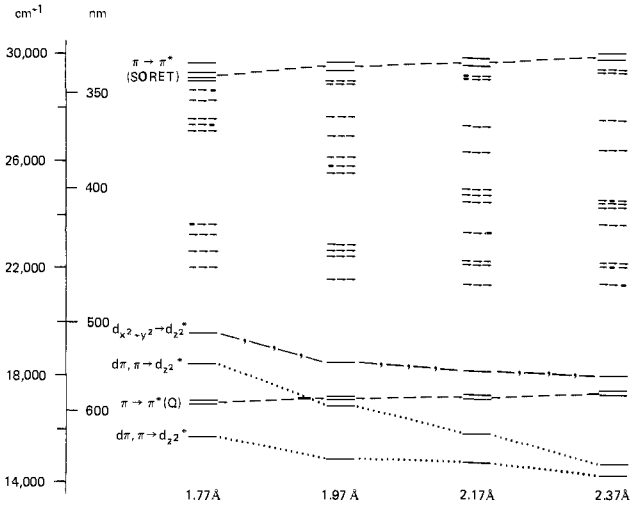

Figure 2. Simplified scaled diagramatic representation of the excited-state energies of the bent carbonylheme complex at iron–carbon distances of 1.77, 1.97, 2.17, and 2,37 Å showing correlation between similar photodissociating states. The $\pi \rightarrow \pi^*$ transitions of the Soret and Q bands are also identified.

calculated optical spectra were shifted toward the red by about 12–15 nm compared to those with iron in the porphyrin plane with the exception of the $d\pi \rightarrow d_{z^2}^*$ and $d_{x^2-y^2} \rightarrow d_{z^2}^*$ transitions which were slightly blue shifted.

Parallel calculations were performed for a bent CO geometry representing carbon monoxyhemoproteins. Since the objective was to study the general effect of bending, only one such geometry, a 45° bend of the C–O bond from the normal axis to the porphyrin plane, was considered. We also calculated the spectra corresponding to kinked and tilted CO geometries, and the results, for the purpose of the present study, were qualitatively in between those of the linear and bent geometries and, therefore, were not pursued further. Table III shows the nature of the ground-state orbitals for the bent carbonylheme complex at iron–carbon distances of 1.77 and 2.37 Å. The calculated excited states below about 30 000 cm^{-1} are given in Table IV for three iron–carbon distances of 1,77, 2.17, and 2,37 Å. A simplified scaled diagramatic representation of the excited-state energies is also shown in Figure 2.

The dramatic difference between these results and those of the linear CO geometry (Table II and Figure 1) is the extensive initial lowering of the energies of the two $d\pi \rightarrow d_{z^2}^*$ states to about 15 700 and 18 000 cm^{-1} at Fe–C = 1.77 Å, due to the bending of CO ligand. The calculated energies of these states are in excellent agreement with the assignment of Eaton et al.[37] of two observed negative and positive circular dichroism bands at 16 000 and 17 850 cm^{-1} (labeled bands I and II) to $d\pi \rightarrow d_{z^2}^*$ transitions. As in the case of the linear carbonylheme complex, these are the only states displaying a dissociative profile, although the overall variation in energy with iron–ligand distance is slightly masked by the initial lowering of their energy due to ligand bending. Other features of the spectra remain the same as in the linear complex. In particular, the two $\pi \rightarrow \pi^*$ transitions, the Q and Soret bands, show a slight increase in energy with increasing iron–ligand distance. Calculation of the excited states with iron out of the heme plane also produced a general red shift of the spectra with the exception of the $d\pi \rightarrow d_{z^2}^*$ and $d_{x^2-y^2} \rightarrow d_{z^2}^*$ transitions which were slightly blue shifted.

We have also calculated the triplet excited states of both linear and bent carbonylheme complexes by using single excitations from the singlet ground state. Figure 3 shows a scaled diagram of the singlet and triplet excited-state energies of both linear and bent complexes at Fe–C distance of 1.77 Å where only the $\pi \rightarrow \pi^*$ and $d\pi \rightarrow d_{z^2}^*$ transitions are identified for clarity. We note that in neither the linear nor bent model complex is the triplet $d\pi \rightarrow d_{z^2}^*$ lowered by more than 4000 cm^{-1} in energy from its singlet

Table III. Ground-State Orbital Descriptions of Bent Carbonylheme Complex at Iron–Carbon Distances of 1.77 and 2.37 Å[a]

orbital no.	Fe–C = 1.77 Å	Fe–C = 2.37 Å
92	(44% Porphσ, 23% Imidσ, 10% d_{z^2}, 7% Porphπ, 5% COσ, 3% COπ)*	(56% d_{xy}, 41% Porphσ)*
91	(72% Imidσ, 23% a_{1u}, 1% d_{z^2}, 1% COπ)*	(64% Imidσ, 14% Porphσ, 14% d_{z^2}, 1% COπ)*
90	(77% a_{1u}, 19% Imidσ)*	(74% a_{1u}, 14% Imidσ, 6% d_{z^2}, 1% COπ)*
89	(59% d_{xy}, 37% Porphσ)*	(38% Imidσ, 26% a_{1u}, 20% d_{z^2}, 9% Porphσ, 2% COπ)*
88	(96% e_g, 3% COπ)*	99% e_g*
87	98% e_g*	99% e_g*
86	(69% COπ, 18% b_{1u}, 6% dπ)*	99% b_{1u}*
85	(84% b_{1u}, 11% COπ, 1% dπ)*	99% Imidπ*
84	(93% Imidπ, 4% COπ)*	(96% COπ, 1% dπ)*
83	(46% Imidπ, 20% COπ, 13% COσ, 11% d_{z^2}, 8% dπ)*	(97% Imidπ, 2% COπ)*
82	99% b_{2u}*	100% b_{2u}*
81	(54% Imidπ, 18% COπ, 12% COσ, 10% d_{z^2}, 4% dπ)*	(43% COπ, 35% COσ, 11% d_{z^2}, 1% dπ)*
80	(99% e_g, 1% dπ)*	(98% e_g, 1% dπ)*
79	(98% e_g, 1% dπ)*	(99% e_g, 1% dπ)*
78	100% a_{1u}	100% a_{1u}
77	97% a_{2u}, 1% COπ	98% a_{2u}, 1% COπ
76	60% dπ, 28% e_g, 3% COπ, 2% d_{z^2}, 2% $d_{x^2-y^2}$	69% dπ, 25% e_g, 1% $d_{x^2-y^2}$
75	61% dπ, 34% e_g, 4% COπ	70% dπ, 29% e_g
74	94% $d_{x^2-y^2}$, 1% dπ	95% $d_{x^2-y^2}$, 1% dπ
73	65% Imidπ, 35% b_{1u}	73% Imidπ, 27% b_{1u}
72	93% a_{2u}, 1% COπ	84% b_{1u}, 14% Imidπ
71	74% b_{1u}, 24% Imidπ, 1% dπ	92% a_{2u}, 1% COπ
70	87% e_g, 6% Imidπ, 5% dπ, 1% COπ	88% e_g, 6% Imidπ, 5% dπ
69	98% e_g	99% e_g
68	76% e_g, 9% Imidπ, 11% dπ, 1% COπ	75% e_g, 13% dπ, 11% Imidπ
67	68% e_g, 23% dπ, 6% COπ	74% e_g, 23% dπ, 1% COπ

[a] Only the orbitals involved in the electronic transitions of below about 30 000 cm^{-1} are shown. Except for iron d and COπ orbitals, all contributions below 5% are neglected. All symmetry designations refer to porphyrin π orbitals in D_{4h} symmetry.

Table IV. Calculated Excited States of Bent Carbonylheme Complex below 30 000 cm^{-1} as a Function of Iron–Carbon Distance

Fe–C = 1.77 Å		Fe–C = 2.17 Å		Fe–C = 2.37 Å	
frequency,[a] cm^{-1}	major components	frequency, cm^{-1}	major components	frequency, cm^{-1}	major components
		14 770	$(d\pi,\pi) \rightarrow (d_{z^2},CO\sigma\pi)^*$ (95%)	14 255	$(d\pi,\pi) \rightarrow (d_{z^2},CO\sigma\pi)^*$ (93%)
15 701	$(d\pi,\pi) \rightarrow (d_{z^2},CO\sigma\pi)^*$ (96%)	15 849	$(d\pi,\pi) \rightarrow (d_{z^2},CO\sigma\pi)^*$ (88%)	14 660	$(d\pi,\pi) \rightarrow (d_{z^2},CO\sigma\pi)^*$ (90%)
16 968 (0.038; xy)	$a_{1u}; a_{2u} \rightarrow e_g^*$ (57%; 40%)	17 211	$a_{1u}; a_{2u} \rightarrow e_g^*$ (59%; 38%)	17 286	$a_{1u}; a_{2u} \rightarrow e_g^*$ (59%; 38%)
17 021 (0.036; xy)	$a_{1u}; a_{2u} \rightarrow e_g^*$ (57%; 41%)	17 261	$a_{1u}; a_{2u} \rightarrow e_g^*$ (58%; 38%)	17 333	$a_{1u}; a_{2u} \rightarrow e_g^*$ (59%; 38%)
18 446 (0.013; z)	$(d\pi,\pi); d_{x^2-y^2} \rightarrow (d_{z^2},CO\sigma\pi)^*$ (57%; 25%)				
19 603 (0.006; z)	$d_{x^2-y^2}; (d\pi,\pi) \rightarrow (d_{z^2},CO\sigma\pi)^*$ (68%; 25%)	18 174	$d_{x^2-y^2} \rightarrow (d_{z^2},CO\sigma\pi)^*$ (91%)	17 922	$d_{x^2-y^2} \rightarrow (d_{z^2},CO\sigma\pi)^*$ (95%)
22 022 (0.003; y)	$d_{x^2-y^2} \rightarrow d_{xy}^*$ (52%); $(d\pi,\pi) \rightarrow e_g^*$ (38%)	21 343	$(d\pi,\pi) \rightarrow e_g^*$ (94%)	21 350	$(d\pi,\pi) \rightarrow e_g^*$ (95%)
22 635 (0.005; y)	$(d\pi,\pi) \rightarrow e_g^*$ (58%); $d_{x^2-y^2} \rightarrow d_{xy}^*$ (36%)	22 107	$(d\pi,\pi) \rightarrow e_g^*$ (95%)	22 072	$(d\pi,\pi) \rightarrow e_g^*$ (95%)
23 247 (0.009; x)	$(d\pi,\pi) \rightarrow e_g^*$ (96%)	22 208	$(d\pi,\pi) \rightarrow e_g^*$ (94%)	22 123	$(d\pi,\pi) \rightarrow e_g^*$ (94%)
23 678 (0.001; xy)	$(d\pi,\pi) \rightarrow e_g^*$ (93%)	23 299	$d_{x^2-y^2} \rightarrow d_{xy}^*$ (90%)	23 597	$d_{x^2-y^2} \rightarrow d_{xy}^*$ (94%)
27 131 (0.003; y)	$d_{x^2-y^2} \rightarrow e_g^*$ (72%); $(d\pi,\pi) \rightarrow d_{xy}^*$ (19%)	24 443	$a_{1u} \rightarrow (d_{z^2},CO\sigma\pi)^*$ (99%)	24 228	$d_{x^2-y^2} \rightarrow e_g^*$ (95%)
27 351 (0.036; x)	$(d\pi,\pi) \rightarrow e_g^*$ (63%); $d_{x^2-y^2} \rightarrow e_g^*$ (24%)	24 754	$d_{x^2-y^2} \rightarrow e_g^*$ (94%)	24 349	$d_{x^2-y^2} \rightarrow e_g^*$ (94%)
27 583	$a_{1u} \rightarrow (d_{z^2},CO\sigma\pi)^*$ (100%)	24 966	$d_{x^2-y^2} \rightarrow e_g^*$ (89%)	24 450	$a_{1u} \rightarrow (d_{z^2},CO\sigma\pi)^*$ (99%)
28 256 (0.010; xz)	$d_{x^2-y^2} \rightarrow e_g^*$ (51%); $(d\pi,\pi) \rightarrow e_g^*; d_{xy}^*$ (22%; 12%)	26 305	$a_{2u} \rightarrow (d_{z^2},CO\sigma\pi)^*$ (50%); $(d\pi,\pi) \rightarrow e_g^*$ (36%)	26 333	$(d\pi,\pi) \rightarrow e_g^*$ (56%); $a_{2u} \rightarrow (d_{z^2},CO\sigma\pi)^*$ (37%)
28 668 (0.158; xyz)	$a_{2u} \rightarrow (d_{z^2},CO\sigma\pi)^*$ (64%); $d_{x^2-y^2} \rightarrow e_g^*$ (12%); $(d\pi,\pi) \rightarrow d_{xy}$ (11%); $a_{1u}; a_{2u} \rightarrow e_g^*$ (3%; 4%)	27 301	$(d\pi,\pi) \rightarrow e_g^*$ (48%); $a_{2u} \rightarrow (d_{z^2},CO\sigma\pi)^*$ (45%)	27 492	$a_{2u} \rightarrow (d_{z^2},CO\sigma\pi)^*$ (60%); $(d\pi,\pi) \rightarrow e_g^*$ (36%)
29 053 (1.611; y)	$a_{1u}; a_{2u} \rightarrow e_g^*$ (30%; 39%); $(d\pi,\pi) \rightarrow d_{xy}^*$ (11%)	29 034	$(d\pi,\pi) \rightarrow d_{xy}^*$ (84%); $a_{1u}; a_{2u} \rightarrow e_g^*$ (3%; 4%)	29 239	$(d\pi,\pi) \rightarrow d_{xy}^*$ (83%); $a_{1u}; a_{2u} \rightarrow e_g^*$ (3%; 4%)
29 102 (0.735; x)	$(d\pi,\pi) \rightarrow d_{xy}^*$ (34%); $a_{2u} \rightarrow (d_{z^2},CO\sigma\pi)^*$ (20%); $a_{1u}; a_{2u} \rightarrow e_g^*$ (13%; 17%)	29 122	$(d\pi,\pi) \rightarrow d_{xy}^*$ (76%); $a_{1u}; a_{2u} \rightarrow e_g^*$ (3%; 4%)	29 319	$(d\pi,\pi) \rightarrow d_{xy}^*$ (78%); $a_{1u}; a_{2u} \rightarrow e_g^*$ (3%; 6%)
29 278 (0.418; xy)	$(d\pi,\pi) \rightarrow d_{xy}^*$ (52%); $a_{1u}; a_{2u}; d_{x^2-y^2} \rightarrow e_g^*$ (8%; 10%; 17%)	29 530	$a_{1u}; a_{2u} \rightarrow e_g^*$ (32%; 46%); $(d\pi,\pi) \rightarrow d_{xy}^*$ (7%)	29 714	$a_{1u}; a_{2u} \rightarrow e_g^*$ (31%; 47%); $(d\pi,\pi) \rightarrow d_{xy}^*$ (9%)
29 657 (1.182; x)	$(d\pi,\pi) \rightarrow d_{xy}^*$ (35%); $a_{1u}; a_{2u}; d_{x^2-y^2} \rightarrow e_g^*$ (19%; 26%; 6%)	29 799	$a_{1u}; a_{2u} \rightarrow e_g^*$ (32%; 46%); $(d\pi,\pi) \rightarrow d_{xy}^*$ (7%)	29 946	$a_{1u}; a_{2u} \rightarrow e_g^*$ (32%; 47%); $(d\pi,\pi) \rightarrow d_{xy}^*$ (8%)

[a] Nonzero oscillator strengths and polarizations are given in parentheses.

partner. It can also be seen from Figure 3a that, in the case of the linear CO geometry, the lowest triplet excited states correspond to the $\pi \rightarrow \pi^*$ transitions of the Q and Soret bands.

Discussion

One major conclusion of the results of this work, as presented in Tables II and IV and Figures 1 and 2, is that, in both linear and bent carbonylheme complexes, representing model compounds and hemoproteins, respectively, only the excited states corresponding to the $d\pi \rightarrow d_{z^2}^*$ and $d_{x^2-y^2} \rightarrow d_{z^2}^*$ display the correct dissociative profile, i.e., decreasing energy with increasing iron–ligand distance and no barrier to dissociation, to be considered as photoactive excited states. Particularly, the lack of dissociative behavior of the $\pi \rightarrow \pi^*$ transitions indicates that the $\pi \rightarrow \pi^*$ states of the Q band cannot be directly photodissociating as has been suggested.[6] The origin of the dissociative behavior of the $d\pi \rightarrow d_{z^2}^*$ and $d_{x^2-y^2} \rightarrow d_{z^2}^*$ states, as shown in Table I and III, is that they involve excitations from bonding and nonbonding into antibonding iron–CO orbitals, respectively.

Another important result of this work is the dependence of the calculated energies of the photoactive states on CO ligand geometry. This dependence could imply important differences in the mechanisms of CO dissociation from hemoproteins compared to model compounds.

Comparison of the calculated excited-state energies of linear and bent carbonylheme complexes at Fe–C = 1.77 Å shows that the energies of the $d\pi \rightarrow d_{z^2}^*$ are lowered from values of about 25 000 and 30 500 cm^{-1} for linear CO geometry (see Table II and Figure 1) to about 15 700 and 18 500 cm^{-1} for bent CO geometry (see Table IV and Figure 2) as a result of the ligand bending. Moreover, the transitions are xy polarized in the linear complex and are z polarized in the bent case. Excellent agreement of the calculated values of the transition energies with the assignment of bands I and II by Eaton et al.[37] is in support of these results. To our knowledge, this is the first report of the calculations of the optical spectra of a model carbonylheme complex with bent ligand geometry. The results clearly show that the singlet $d\pi \rightarrow d_{z^2}^*$ state energies are lowered to the same range as that of the Q-band $\pi \rightarrow \pi^*$ transitions as a consequence of Fe–C–O bending. A similar lowering was also obtained for the $d_{x^2-y^2} \rightarrow d_{z^2}^*$ state. On the basis of these results, therefore, excited singlet states involving $d\pi \rightarrow d_{z^2}^*$ and $d_{x^2-y^2} \rightarrow d_{z^2}^*$ transitions in the bent carbonylheme complex have both the correct dissociative profile and the energy range to account for the observed broad region of wavelength-independent high quantum yield, which extends to the low excitation frequency of about 16 000 cm^{-1}.

The situation is more complicated in the case of the linear carbonylheme complex. Here, although the states corresponding to the $d\pi \rightarrow d_{z^2}^*$ and $d_{x^2-y^2} \rightarrow d_{z^2}^*$ transitions are again the only two states displaying the correct dissociative profile, their energies are too high to account for the low excitation frequency limit[14] and the high quantum yield[5] also observed in CO photodissociation of model heme compounds. One possible explanation is that deviations from the linear geometry of model compounds seen in the crystallographic structures[53,54] may occur under the experimental conditions employed in the photodissociation studies. That

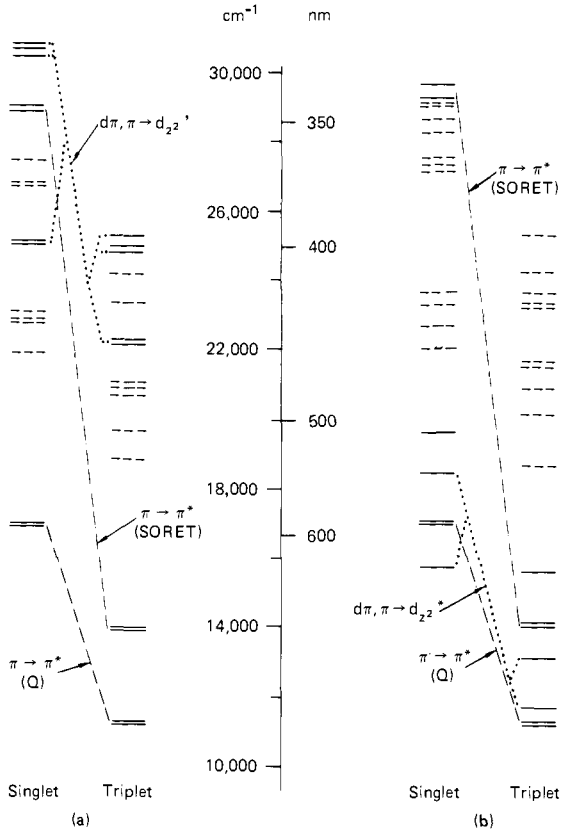

Figure 3. Scaled diagram of the singlet and triplet excited-state energies of the linear (a) and bent (b) carbonylheme complexes at iron–carbon bonding distance of 1.77 Å. Only the states corresponding to the $\pi \rightarrow \pi^*$ and $d\pi,\pi \rightarrow d_{z^2}^*$ transitions are identified.

is, some degree of bending of the CO ligand in model compounds and protohemes could be responsible for lowering of the energies of the photoactive excited states, thereby resulting in the observed photodissociation properties. Our own calculations[45] and those of others[41] show that the potential surface for CO bending mode is very soft in carbonylheme complexes. Careful studies of the temperature dependence of the quantum yield and its wavelength dependence in CO photodissociation from model compounds, at low temperatures, should help resolve this question.

On the basis of the results of the calculations of the excited singlet states at the single CI level, we suggest the following mechanism for CO photodissociation. We identify the $d\pi \rightarrow d_{z^2}^*$ state as the main photodissociating state in both carbon monoxyhemoproteins and model compounds because of its dissociative profile as a function of iron–ligand distance, its bonding to antibonding excitation character, and its nonzero oscillator strength. The $d_{x^2-y^2} \rightarrow d_{z^2}^*$ state may also be directly involved in photodissociation but, due to its zero oscillator strength, the degree of its contribution cannot be assessed with certainty. However, it, too, has the correct dissociative character in terms of energy behavior and of involving nonbonding, $d_{x^2-y^2}$, to antibonding, d_{z^2}, orbital excitations to also contribute to the enhancement of photolability. CO photodissociation can thus occur either by direct excitation into the $d\pi \rightarrow d_{z^2}^*$ states or by $\pi \rightarrow \pi^*$ excitations followed by decay into these states.

It should be emphasized that all these calculations were performed with the assumption that Fe–C bond breaking is the first event of the photodissociation process and can occur in a frozen, $S = 0$, spin state and conformation. The "frozen spin state" assumption is a reasonable one, at least in the time scale of less than 30 ps, during which, according to resonance Raman studies,[30,31] the heme spin state may change to $S = 2$. The time scale for the out-of-plane movement of iron has remained uncertain.[27,28,30,31] The recent ps Raman spectra[30,31] of the HbCO photointermediates have been interpreted in terms of increased heme core size. However, according to the authors, some out-of-plane displacement of the iron is allowed by the uncertainty in the data, and the iron may be at an intermediate position on the reaction coordinate between HbCO and Hb.[31] If this out-of-plane displacement of iron is real and precedes the spin state change, our calculated red shift of the optical spectra by 12–15 nm for 0.24-Å displacement of the iron may be used to predict a similar red shift, though possibly less in magnitude, for the photointermediate observed within 4–6 ps after photodissociation.[22] It may also provide a partial explanation for the observed red shift of photointermediates which have been interpreted in terms of Hb-like spectrum.[25,26]

An important question in the photodissociation of CO is the involvement of the triplet $d\pi \rightarrow d_{z^2}^*$ state through intersystem crossing from a singlet $d\pi \rightarrow d_{z^2}^*$ or other excited states. Our results argue against the necessity of involving triplet states to account for activation of photodissociation at *Q*-band energies. As shown in Figure 3a, the lowest triplet states correspond to nondissociating $\pi \rightarrow \pi^*$ states and the triplet $d\pi \rightarrow d_{z^2}^*$ lies above the singlet $\pi \rightarrow \pi^*$ (Q) states in energy. Figure 3b shows that, in the case of bent CO geometry, the singlet $d\pi \rightarrow d_{z^2}^*$ is already a low energy state below the Q band that can be populated either by direct excitation from the ground state or by decay from higher order singlet excited states.

While intersystem crossing is not necessary to account for initiation of photodissociation, our results are entirely consistent with its occurence as one of the later events of photodissociation resulting in rapid spin conversion in the excited state[31] and possibly an intermediate species with spin $S = 1$ before relaxing to deoxy ($S = 2$) state.[21] From comparison of Figure 3, a and b, it can be deduced that the rate of intersystem crossing may be sensitive to small variations in ligand bending angle which may in turn be protein dependent. It can also be argued that variations in the rate of intersystem crossing may affect the rapid ligand recombination rate due to the spin change of the heme. Thus there may be a causal link between the nature of the protein and the ligand recombination rate via the ligand geometry and the intersystem crossing rate. This provides another interpretation for different quantum yields in MbCO and HbCO which has been explained in terms of geminate ligand recombination.[24,29]

Conclusion

The results of the single configuration interaction calculations of the excited-state energies of carbonylheme complexes as a function of iron–ligand distance definitively establishes that the $d\pi \rightarrow d_{z^2}^*$ state is the photodissociating excited state. It is concluded that the observed photodissociation features of carbon monoxyhemoproteins such as high quantum yield and its wavelength independence over the frequency range of 16 000–33 000 cm^{-1} are inherently related to the bending of the C–O bond from the axis normal to the heme porphyrin plane. Similarities in the photodissociation properties of the carbonylhemoproteins and the corresponding model compounds can be explained in terms of the soft potential surface of the ligand bending mode in the model compounds. It is predicted that photodissociation of a strictly linear CO ligand observed in crystallographic studies on model compounds would occur at higher excitation frequencies. Careful temperature and wavelength dependence study of the model compounds are needed to confirm the role of the ligand geometry. Photodissociation of CO can occur by either direct excitation into singlet $d\pi \rightarrow d_{z^2}^*$ state or higher order excitations followed by decay into this state. The triplet $d\pi \rightarrow d_{z^2}^*$ need not be invoked on energetic grounds, and the intersystem crossing into this state, if any, could be one of the later events of photodissociation presumably related to the change in the spin state of the heme.

Acknowledgment. We gratefully acknowledge financial support for this work from NSF Grant PCM 7921591. We are also grateful to Drs. Marvin M. Makinen and Antonie K. Churg for bringing the problem to our attention, Dr. Marie-Madeleine Rohmer for participation in the initial phases of this study, and Dr. Dale Spangler for many helpful discussions during the course of this work. We further wish to thank Wanda Davis and Brenda Wells for their help in the preparation of the manuscript.